



Hysteresis and Related Magnetic Studies on Zn & Sb Substituted Cu Ferrites in Relation to Verwey's Hopping Transition Mechanism

R.Dhanaraju^a, M.KRaju^a, V.Brahmajirao^b, S.Bangarraju^a

^aMaterial Science Research Laboratories & Central Instrumentation Facility, Department of Physics, Andhra University, Visakhapatnam-530005., INDIA.

^bDept. of Nano science and Technology, School of Biotechnology, MGNIRSA, D.Swaminathan Research Foundation,[DSRF] Gaganmahal, HYDERABAD-500015, INDIA

ABSTRACT

This paper is concerned with the experimental investigation about of the electronic structure of a number of Nano Crystalline Insulating Transition Metal (NCITM) compounds, in the light of Hubbard's model & Verwey's Hopping Transition Mechanism(VHTM), as detailed by Hidetoshi Fukuyama[6] in his review in the light of Hysteresis studies. Two series $(\text{Cu}_x \text{Zn}_{(1-x)} \text{Fe}_2 \text{O}_4)$ and $(\text{Cu}_{(1-x)} \text{Sb}_2 \text{Fe}_2 \text{O}_4)$ for $(x= 0.0 \text{ to } 1.0)$ in steps of 0.2, for 'x' are Synthesized, by the conventional ceramic method. The single-phase cubic spinel structures of the samples were confirmed by x-ray diffraction patterns. Our earlier reported Morphological studies using SEM, Structural studies using XRD, Electrical conductivity studies, using Hewlett Packard 4192A impedance analyzer, FTIR studies, using BRUKER (ALPHA) FT-IR system with OPUS 6.5 (version) software, support the findings of the present Hysteresis and related magnetic studies done in our Material science research laboratories. Results are interpreted in the light of VHTM and related models. Very recent Concurrent findings from literature are cited.

Keywords: Verweys Hopping Transition Mechanism, Doped Cu-Zn-Sb Ferrites, Hysteresis, Hubbard's model, Doped Nanoferrites, Electrical studies, Magnetic & FTIR, studies, Morphology & structural studies, ceramic & solid-solution synthesis of Doped Ferrites

1. INTRODUCTION

Cu-Zn ferrites are suitable to be used in switching devices due to their spontaneous rectangular hysteresis loops behavior with high rectangular ratio [1, 2]. Even after 2000 years of the discovery of magnetism, still there are challenges from it and more so with the advent of the Nano science, in spite of many a unspared effort, to unravel its exciting characteristics that are in progress. [3]. J.M.Fert & G.Grunberg., discovered the Giant Magneto Resistance (GMR) effect [4], that opened the window for an efficient control of the motion of the electrons, by acting on their spin through the orientation of of a magnetization. Two of the simplest theoretical models that are widely used in a qualitative or a semi-quantitative way are the Hubbard Hamiltonian [5], used for studying the interplay between electron delocalization and electron repulsion effects, and the Anderson model[6] for the understanding of a magnetic impurity coupled to a conduction band. Model Hamiltonian investigations can often describe tendencies and reveal the basic mechanisms of various physical phenomena. At the same time the model Hamiltonian approach is rather limited in its ability to make quantitative predictions.[7] since even the simple Hubbard model can be solved exactly only in

the one-dimensional case. In dealing with the two- and three- dimensional models numerical techniques are usually employed, based on quantum Monte Carlo methods [8] or on diagonalizing the Hamiltonian for a cluster of atoms. However, the quantum Monte Carlo methods suffer from the so-called sign problem, while the exact diagonalization is limited by the exponential growth of the computational effort with the cluster size [9]. A systematic understanding of electronic properties is now possible, in spite of apparently complicated crystal structures. Yu-Wei Su[16], in his thesis on fabrication of a magnetic film between the coplanar transmitted strip line for crosstalk suppression, used Screen printing to fabricate yttrium iron garnet ($\text{Y}_3\text{Fe}_5\text{O}_{12}$) films replacing ferrite plated zinc ferrite films, because of the magnetic properties of yttrium iron garnet film. The results show that screen-printed films can achieve far-end crosstalk suppression by 10 ~ 12dB.

Low permeability (μ), low saturation magnetization (M_s) high resistivity (ρ) and low eddy current losses are characteristic properties of Cu-Zn ferrite. The procedure or method adopted for preparation of Cu-Zn ferrite also influences the physical parameters. Adding substituent cations in a basic ferrite is an established method to

improve the values of the physical properties. Investigations for possible enhancement of M_s , T_c , μ_i with low magnetic loss factor H_{\square} are required for the development of materials for applications in magnetic recording devices and also for low frequency to higher and microwave frequency applications. Substitution of Sb^{5+} cations is done to study the variation of saturation magnetization (M_s) and Curie temperature (T_c) as a function of substituent concentration. Compositional and frequency dependence of initial permeability (μ_i) along with magnetic loss factors (H_{\square}) is also investigated besides the hysteresis studies.

2. EXPERIMENTAL: METHODS AND MATERIALS

Two series ($Cu_x Zn_{(1-x)} Fe_2 O_4$) and ($Cu_{(1-x)} Sb_2 Fe_2 O_4$) for ($x=0.0$ to 1.0) in steps of 0.2 for 'x' are chosen for our studies. The conventional ceramic method [14, 15 & 16] is used for the preparation of the samples of the chosen series. Highly pure (analytical reagent grade) CuO , $Fe_2 O_3$ and $Sb_2 O_5$ and ZnO chemicals were used. The details of the method of synthesis were shown in the flowchart and are also available elsewhere [17, 18, and 19]. Suitable temperature is required to perform solid state reaction among constituent oxides of the mixed ferrite to be formed. These samples were used to obtain the data in systematic Morphological studies [18] using SEM, of *JEOL*, make model *JSM-840*; Structural studies using XRD *Philips* Diffractometer (model *PW-3710*) Setup; Electrical conductivity studies [17] using *Hewlett Packard 4192A* impedance analyzer(photos shown below) & FTIR studies [19] using *Bruker (ALPHA) FT-IR system with OPUS 6.5 (version) software*. Since the mechanical grinding cannot give particles of uniform size and shape the homogeneity, morphology and microstructure of the material are affected in such a method. The single-phase cubic spinel structures of the samples were confirmed by x-ray diffraction patterns.

The lack of retrace ability of the magnetization curve is known as hysteresis. It is concerned to the existence of magnetic domains in the material. Once the magnetic domains are aligned in certain direction, it takes some energy to turn back to its original position. The hysteresis curves for these samples are shown (in the Plots 1 to 12) Fursina [20], in his studies on a novel mechanism called Electric Field Driven transition (EFD), presented in the Ph.D., thesis (to Rice University, Houston, Texas, 2010, U.S.A), on magnetite, reported strong evidences about transition from high- to low-resistance states, driven by application of high bias. This transition is detected both in $Fe_3 O_4$ nanoparticles and thin films, and is hysteretic in voltage under continuous biasing, and is not caused by self-heating

E Manova [21] prepared Nickel zinc ferrite nanoparticles, $Ni_{1-x} Zn_x Fe_2 O_4$ ($x = 0, 0.2, 0.5, 0.8, 1.0$), with dimensions below 10 nm by combining chemical precipitation with high energy ball milling, and studied their analogues obtained by thermal synthesis for comparison, Mössbauer spectroscopy, X-ray diffraction, and magnetic measurements are reported. X-ray diffraction shows that after 3h of mechanical treatment ferrites containing zinc are formed, while 6h of treatment is needed to obtain $NiFe_2 O_4$. The magnetic properties of the samples exhibit a strong dependence on the phase composition, particle size and preparation method.

S. Deka et.al. [22] Synthesized Nano crystalline $Ni_{0.5} Zn_{0.5} Fe_2 O_4$ with average particle size of 9 nm by auto combustion method and characterized the Magnetic properties. Mei Yu et.al., [23] fabricated Highly ordered nanowire/tube arrays of $Ni_{0.5} Zn_{0.5} Fe_2 O_4$ by the sol-gel method in the pores of anodic alumina membrane SEM, TEM, and XRD studies are reported. R. L. Dhiman et .al. [24] prepared Aluminum doped manganese ferrites by the double ceramic route and confirmed the formation of mixed spinel phase by X-ray diffraction analysis. They established from the spectral analysis of Mossbauer spectra that Al^{3+} ions replace iron ions at B-sites. This change in the site preference reflects an abrupt change in magnetic hyperfine fields, at A- and B-sites as aluminum concentration increases, which has been explained on the basis of super transferred hyperfine field.

3. RESULTS AND DISCUSSION

Systematic hysteresis studies conducted on the above Zn & Sb doped Cu ferrites, synthesized in our Material science research laboratories of Andhra University, Visakhapatnam., were used and the results of the Magnetic studies namely: (1) the hysteresis data, as plots (2) the variation of magnetic loss factor ($\tan \mu_i$) with additive concentration.(3) Evaluated domain wall energy per unit area as a function of substituent concentration, are reported here. Our results find concurrency in findings with those cited from literature. The data about Evaluated Domain wall energy per unit area as a function of substituent concentration, and The variation of magnetic loss factor ($\tan \mu_i$) with additive concentration, are given in Tables (1) and (2). Initial permeability (μ_i) and grain size (Dg) are two important parameters used to evaluate quality and behavior of a ferrite. During recent years non-magnetic grain boundary (NMGB) model [26] is given due importance over Globus model. However, for larger grains Globus model could be adopted to understand microstructure of the material. Globus et al [27] pointed out that domain wall bulging would still permit wall movement even while the end points were tied down. The domain walls bulge under application of

magnetic field until a critical field H_{cr} causing the wall to get unpinned. According to this model the domain wall Energy per unit area (γ) is calculated using the formula: $\{(\mu_i - 1) = (3 M_s^2 D_g) / 16 \gamma\}$, Where M_s is saturation magnetization, D_g is grain diameter, μ_i is the initial permeability. The evaluated values are given in Tab 5.1. The substitution of Sb^{5+} or Zn^{2+} is led to the increase of domain wall energy with substituent concentration up to ($x = 0.20$). For further concentration it is found to decrease. Low concentration of substituent with the increased domain wall energy is suitable to induce driving force for the movement of grain boundary resulting increase in grain size. The decrease of γ at higher concentrations of substituents depicts its small contribution for grain growth because of the undetected impurity phase that formed. Variation in ' M_s ' are generally explained on the basis of modified exchange interactions due to preferential site occupancy of the substituent ions and host lattice cations. According to Neel [2], in ferrites, there are three kinds of exchange interactions between unpaired electrons of two ions (a) lying Both in A sites (A-A interaction) (b) Both in B sites (B-B interaction) and (c) In A and B sites (A-B interaction) : Hence the net magnetization (M) can be written as: $\overline{M} = \overline{M}_A - \overline{M}_B$, Where \overline{M}_A the magnetization of A is sublattice and \overline{M}_B is the magnetization of B sublattice. Earlier in neutron diffraction studies of $Fe^{3+} Sb^{5+}$ configuration was reported [34] as ferromagnetic coupling between Fe and Sb sublattices resulting $M_s = 4 \mu_B / f.u$ since Fe^{3+} and Sb^{5+} have $3d^5$ and $4d^1$ electronic configurations respectively. Later in the studies have a similar value was reported [35] for Fe^{2+} and Sb^{5+} configuration with ferromagnetic coupling between Fe^{2+} ($3d^6$) and Sb^{5+} ($4d^0$) ions. For the latter coupling, the determined magnetic moment values of Fe and Sb ions are $\mu_{Fe} = 4.0 \pm 0.1 \mu_B$, $\mu_{Sb} = 0 \pm 0.1 \mu_B$ respectively, which was consistent with the observed $\mu_{Fe} = 4.0 \mu_B$. The exchange interactions (A-A) or (B-B) are weak compared to A-B interactions. Hence, it must be in the form of $Fe - O - X$ [36, 37] resulting large hybridization of the orbitals and $Fe-X$ band plays role in exchange interaction [38]. By substitution of Sb/Zn in Mn-Zn ferrites at small concentrations slight increase of M_s was reported for Sb substituted ferrites while M_s decreased for other concentrations of Sb and Zn [39]. It is well known fact that substitution of small concentrations of paramagnetic ions results in increase of saturation magnetization [1]. To understand the observed variation in saturation magnetization, the following possibilities are to be considered for different substituent concentrations. (1) Zn^{2+} / Sb^{5+} ions occupy A sites replacing A sites iron ions. Hence M_A decreases, if Cu^{2+} ions partially begin to occupy B sites, causes increase of M_B . Eventually net magnetization increases significantly. (2) Zn^{2+} / Sb^{5+}

may occupy both A and B sites in unequal concentrations. Added Cu^{2+} ions occupy B sites replacing Fe^{3+} ions with decrease of M_A and M_B (3) Zn^{2+} / Sb^{5+} ions may partially replace A site Fe^{3+} ions and partially push Cu^{2+} ions to B sites decreasing M_A and increasing M_B is also due to presence of Cu^{2+} ions. The observed M_s (10.91 emu/gm) for the basic ferrite is in agreement with the reported value (11.6 emu/gm) [9]. At lower concentrations of substituents, the tetrahedral sites are occupied by substituent cations causing tetrahedral (A) sub lattice magnetization to decrease and hence the resultant magnetization increases. At higher concentrations of substituents, Zn^{2+} / Sb^{5+} occupy B sites replacing Fe^{3+} ions. Magnetization of B sub lattice decreases and hence net magnetization decreases.

At higher concentrations ($x \leq 0.2$) substituent ions distribute among A and B sites magnetization of A and B sub lattices would decrease and net magnetization decreases effectively with increased substituent concentration till $x = 0.40$. But small values of saturation magnetization materials substituted with high substituent concentration confirm the above model of cation distribution. This show at higher concentrations, these substituents partly occupy B sites replacing Fe^{3+} ions and partly occupy 'A' sites replacing other cations satisfying local charge neutrality condition. This results in considerable decrease of saturation magnetization.

Earlier for Li-Zn ferrites linear relationship between μ_i and D_g was observed with the addition of Sb_2O_5 [20]. This linearity was interpreted by the Globus model [28]. According to this model the relation between D_g and μ_i was explained based on bulging of domain walls that exist inside the grains. If the formed grains are free from the pores and defects, then a plot of D_g versus μ_i , in general exhibits a linear relationship. Deviation from linearity due to microstructural effects reflects on the quality of the ferrite. μ_i , and D_g are found to follow linear relationship for Mo substituted ferrites while in the case of Sb added ferrites correlation between μ_i , and D_g is not observed.

Kadam G.B., et.al. [27], prepared polycrystalline ferrite samples having the general formula.

$(Co_{(1-x)} Zn_x Fe_{(2-y)} Sm_y O_4)$ (Where $x = 0.0, 0.1, 0.2, 0.3, 0.4, 0.5$ and $y = 0.05$) by conventional standard ceramic technique. The single-phase cubic spinel structures of the samples were confirmed by x-ray diffraction patterns.

They reported that substituted Sm^{3+} decreases the lattice constant by small extent and increases x-ray density. Lattice constant was found to decrease first up to $x = 0.1$, beyond which it increased with Zn concentration x .

The x-ray density was found to increase first up to $x=0.1$ and then after it decreased slowly. The hopping lengths L_A , L_B and bond lengths d_{Ax} , d_{Bx} were found to vary as per changes in lattice constant. The cation distribution showed that non-magnetic (Zn^{2+}) occupied *A-site*, (Ni^{2+}) and (Sm^{3+}) were found to be diverting towards *B-site*. Lattice constant calculated theoretically from cation distribution was found to be higher than experimentally observed lattice constant. The substitution increased the electrical resistivity of ferrites and the resistivity decreased with increasing temperature. The graphs between ($\log \rho$) and ($1000/T$) showed two regions corresponding to paramagnetic and Ferromagnetic behavior through straight lines. Curie temperature obtained by d. c. resistivity was in good compromise with those obtained by a. c. susceptibility. Activation energies are found to be greater in paramagnetic region than those in ferromagnetic region. All these observations are in good tune with those of ours.

Shenghui Guo, et.al. [11] attempted to utilize fused zirconia to prepare partially stabilized zirconia using roasting process. Effects of roasting temperature and holding time on the specific polymorphic phase transition of fused zirconia were systematically analyzed, and microstructure of fused zirconia before and after roasting process were obtained and characterized by XRD and SEM, respectively. The characterization results showed that untreated fused zirconia Mainly consists of crystalline compounds of cubic ZrO_2 phase; while the roasted one mainly was composed of crystalline Compounds of cubic ZrO_2 phase and monoclinic ZrO_2 phase. Partially stabilized zirconia had to have a big acicular Pattern crystal grains and finely ground particles gathering at the crystal boundary. Cubic ZrO_2 phase of fused zirconia is partially converted into monoclinic ZrO_2 phase at roasting temperature of 1723 K for 240 min Pathan.A.N, et.al. [12], synthesized Nano crystalline [$Co_{0.4}Zn_{(0.4-x)}Cu_xFe_2O_4$] by the co-precipitation Method, and their XRD findings established that the spinel ferrite retaining some hydroxyl groups was formed. Nanoparticles with average particle size of 10–100 nm were obtained by sintering the samples between 393 and 1173 K. Saturation magnetization of the samples increased with increasing average particle size up to 11 nm and for samples with particle, size >11 nm, the saturation magnetization decreased with increasing particle size. This was attributed to a change in cation distribution with change in particle size. To understand the magnetic nature of the cubic ferrite phase formed at a temperature as low as 80°C, (Fe-57) Mossbauer spectra were recorded for samples annealed at three different temperatures, without any external magnetic field, and with an external field of $H_{ext} = 5$ T, at 4.2 K. The spectral parameters at room temperature, namely, isomer shift, quadruple splitting and

hyperfine field, confirmed the presence of ultrafine super paramagnetic crystallites of Ni-Zn ferrite. The Mossbauer spectra at 4.2 K revealed spin relaxation effects resulting in very broad sextets, characteristic of ultrafine crystallites. The Mossbauer spectra recorded showed well-resolved two-sextet pattern with characteristic hyperfine interaction parameters of the cubic ferrite phase. The Mossbauer studies with our samples are in progress and the results would be communicated soon. Kadam G.B., et.al. [13] Studied the electrical and magnetic behavior of ferrite system [$Ni_{(1-x)}Zn_xFe_{(2-y)}Eu_yO_4$] as a function of temperature, by means of d. c. resistivity and a. c. susceptibility measurements. D.C. resistivity increased after substitution of Eu^{3+} . Curie temp obtained graphically for this system was found to decrease with increase in Zn concentration 'x', which was supported by the a. c. susceptibility measurements. Curie temperatures obtained from d. c. resistivity measurement and a. c. susceptibility measurements showed good agreement, and showed a decrease due to Eu^{3+} substitution. We came across a similar set of conclusions in our studies that were already reported, elsewhere.

R.N. Bhowmik et.al.,[28] synthesized the composition of $Fe_{3(1-x)}Co_{3x}O_4$ for ($x = 0.1, 0.3$ and 0.5) spinel ferrite using the techniques of mechanical alloying, high temperature annealing of milled samples and conventional solid state sintering, and comparative results of the crystal structure formation and dielectric properties of the materials studied at room temperature were presented. The crystalline structure of the single phased samples was cubic spinel phase with space group $Fd\bar{3}m$. The alloying of two spinel oxides was also complemented from FTIR spectrum. Impedance spectroscopy suggested only one semi-circle in the Cole-Cole plot of mechanical milled samples, which indicated the dominant grain boundary contribution in the conduction Mechanism. In addition to the grain boundary contribution, the electrical conduction from grains was also substantial in the single Phased compositions of their materials.

A.M.Bhavikatti [29], prepared $NiFe_2O_4$ (Nickel ferrite) by microwave synthesis using urea as a fuel. Nickel oxalate and iron oxalate were irradiated with microwaves in the presence of fuel to get nickel Ferrite, on which **Dielectric and Conductivity measurements** were reported. Microwave method being clean and non-polluting these findings would be conspicuous. The dielectric properties and ac conductivity (σ_{ac}) studied for the prepared sample in the temperature range 00-7000 C and for different frequencies 1 KHz, 10 KHz, 100 KHz and 1MHz. revealed a semiconductor behavior with temperature. The dielectric behavior is explained by using the mechanism of polarization process. The **Magnetic measurements** on nickel ferrite were carried out by using

a vibrating sample magnetometer in the applied field 958.68 Oes at room temperature. The H_c values confirmed that hard ferrites were obtained by this Procedure. D.C Conductivity measurements were carried out on the nickel ferrite by using an electrometer in the temperature range from 260 C to 4000 C.

C. Venkataraju et.al.,[30] synthesized Nano-particles of $Mn_{(0.5-x)}Ni_xZn_{0.5}Fe_2O_4$ ($x = 0.0, 0.1, 0.2, 0.3$ and 0.5) by chemical co-precipitation method. The lattice constant of the octahedral sites was estimated. The dielectric constant decreases with the increase in Ni concentration except for $x = 0.3$. Relaxation peaks were observed for all increases in temperature.

Carolyn I. Pearce et.al, [31] studied Ordering of Fe^{3+} and Fe^{2+} between octahedral (Oh) and tetrahedral (Td) sites in synthetic members of the magnetite (Fe_3O_4) – ulvöspinel (Fe_2TiO_4) solid-solution series, by the determination using Fe $L_{2,3}$ -edge *X-ray magnetic circular dichroism (XMCD)* coupled with electron microprobe and chemical analysis, Ti L -edge spectroscopy, Fe K -edge EXAFS and XANES, **Fe-57 Mossbauer spectroscopy** and unit cell parameters. Microprobe analysis, cell edges and chemical **Fe O** determinations showed that the bulk compositions of the samples were stoichiometric magnetite-ulvöspinel solid solutions. Surface sensitive XMCD showed that the surfaces of these oxide minerals were more sensitive to redox conditions and some samples required re-equilibration with suitable solid-solid buffers. Detailed site-occupancy analysis of these samples gave **XMCD- (Fe^{2+}/Fe^{3+})** ratios very close to stoichiometric values. $L_{2,3}$ -edge spectroscopy showed that Ti^{4+} was restricted to Oh sites. **XMCD** results showed that significant Fe^{2+} only entered **Td** when the **Ti** content was > 0.40 apfu while Fe^{2+} in Oh increased from 1 a.p.f.u in magnetite to a maximum of ~ 1.4 apfu in USP45. As the Ti content increased from this point, the steady increase in Fe^{2+} in Td sites was clearly observable in the XMCD spectra, concurrent with a slow decrease in Fe^{2+} in Oh sites. Calculated magnetic moments showed a steady decrease from magnetite (4.06 μB) to USP45 (1.5 μB) and then a slower decrease towards the value for ulvöspinel (0 μB). Two of the synthesized samples were also partially maghemitized by re-equilibrating with an oxidizing **Ni-Ni O** buffer and XMCD showed that Fe^{2+} oxidation only occurred at Oh sites, with concomitant vacancy formation restricted to this site. This study shows the advantage of

using XMCD as a direct measurement of Fe oxidation state in these complex magnetic spinel's.

S.R. Sawant et.al.,[32] observed that Magnetisation for both slow cooled and quenched samples of $Cu_xZn_{1-x}Fe_2O_4$ as a function of Zn content has shown a maximum at $x = 0.6$ and a decrease for $x > 0.6$. The increase of magnetisation was explained on the basis of Neel's two sub-lattice model while the decrease of magnetisation was explained on a three sub-lattice model. Quenched samples showed higher magnetisation than the slow cooled ones and this increased with the increase of temperature of quenching. The cation transfer between the two sites, characteristic of the temperature that can be frozen-in seems to govern this. Variation of M_r/M_s with the content of Zn for both slow cooled and quenched samples indicated more impedance to the domain wall motion or higher Zn content. As the temperature of quenching was increased M_r/M_s decreased and this was attributed to detect cluster formation. Shun Hua Xiao et.al., [33] prepared Cobalt ferrite ($CoFe_2O_4$) nano powder by a low-temperature, auto-combustion method and studied its thermal evolution of the precursor, the microstructure, morphology and magnetic properties. The report that the synthetic process was a thermally induced redox reaction with carboxyl group as reductant and NO_3^{-1} ions as oxidant. The grains observed in as-burnt powder were proved to be $CoFe_2O_4$ nano crystallites with high dispersibility and low agglomeration. Both the saturation magnetization (M_s) and the remnant magnetization (M_r) were found to be highly depending upon the annealing temperature. The highest coercivity (1373 Oe) was achieved by the sample annealed at 400 °C & their results indicate that the method might provide a promising option for synthesizing high-quality $CoFe_2O_4$ Nano powder.

ACKNOWLEDGEMENTS

The author^a records his thanks to Dr. Malivel Raja, Scientist, DMRL, of DRDO, Hyderabad., A.P., INDIA, for several valuable discussions and suggestions during the course of the work. The authors^{a,b,c} also thank Dr. N.S.Naidu, and Dr. K.Trinadh, Scientists of Naval Science and Technological Laboratories, Visakhapatnam,A.P., INDIA, for their valuable help and suggestions in providing help to use their facility and planning the work to take measurements .One of the authors (R. Dhanaraju), records thanks to UGC , for the fellowship with which this work could be done .

Photographs of (a) Bruker (ALPHA) FT-IR System, (b) Philips XRD Diffractometer Apparatus Model PW-3710



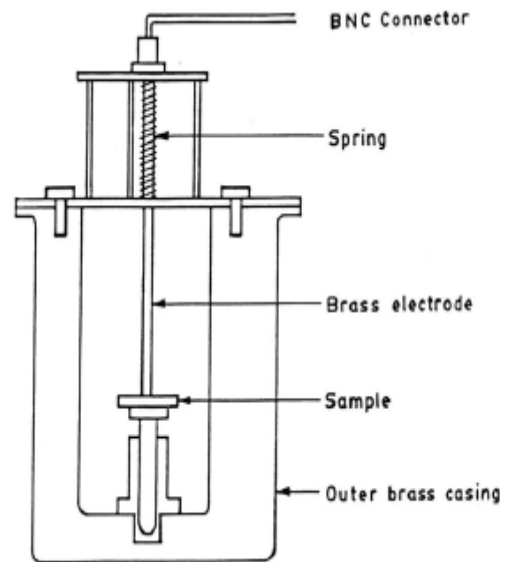
(a)



(b)



(c)



(d)

Photographs of (c) Scanning Electron Microscope [JEOL model JSM-840] ,at Material Science Research laboratories, Andhra University ,Visakhapatnam-530003, INDIA , & (d) Cell used in the Resistivity Measurement



Hysteresis Loop Tracer (Imagetronics)

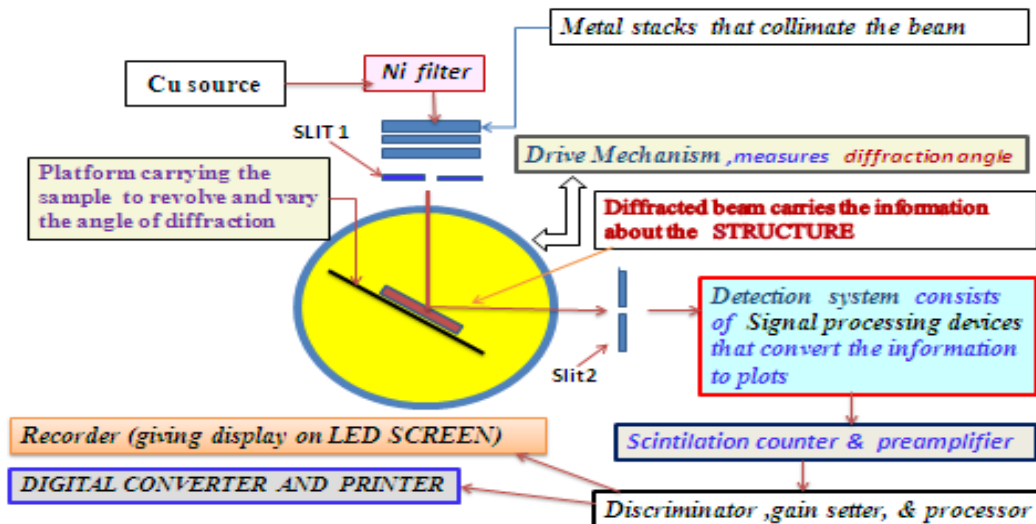


Impedance Analyser 4192A

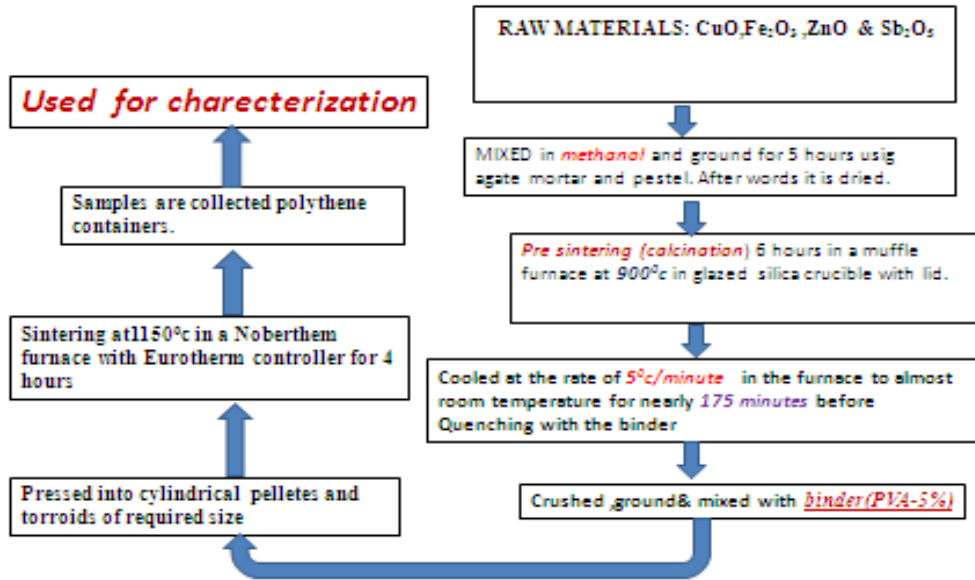
5Hz - 13 MHz

Photographs of: Hysteresis Loop Tracer of Imagetronics and Hewlett Packard 4192A Impedance Analyzer

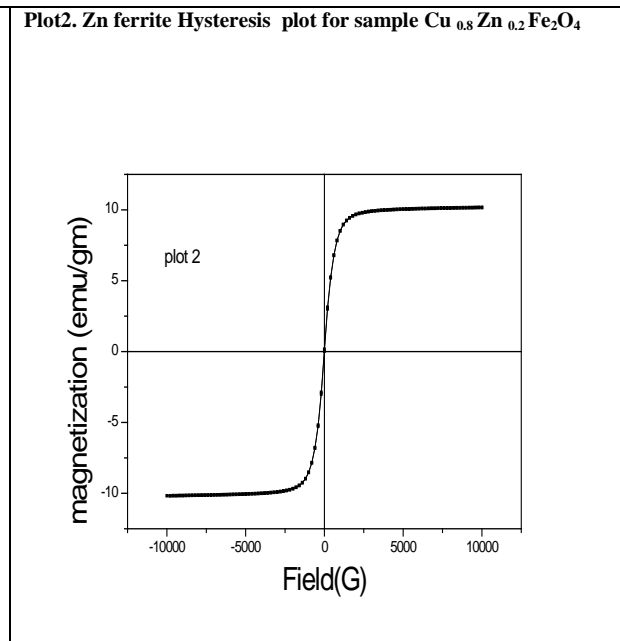
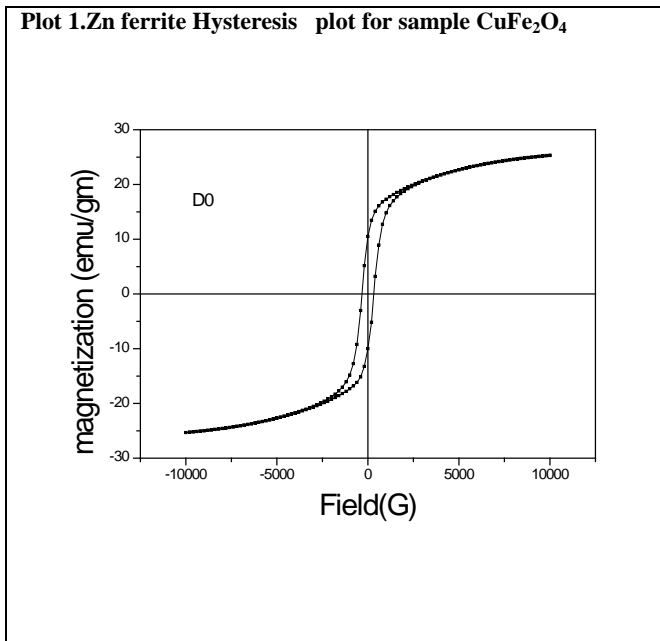
Block diagram of X-ray Diffraction Set up of XRD



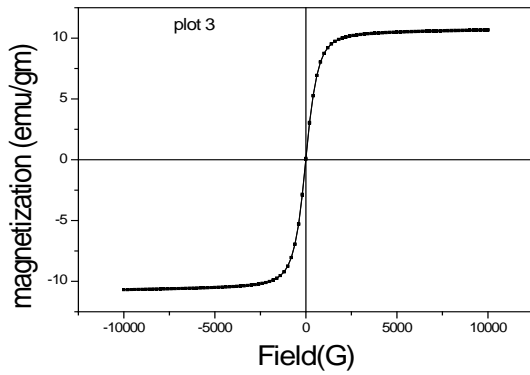
FLOW CHART FOR FERRITE PREPARATION



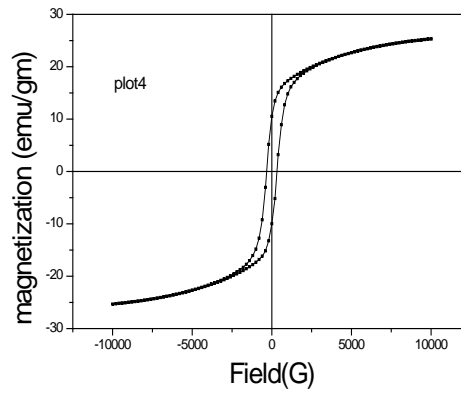
Plot1 to Plot 12 : Field (in G) vs. Magnetization (emu/gm) (Hysteresis)Plots for Zn and Sb doped samples



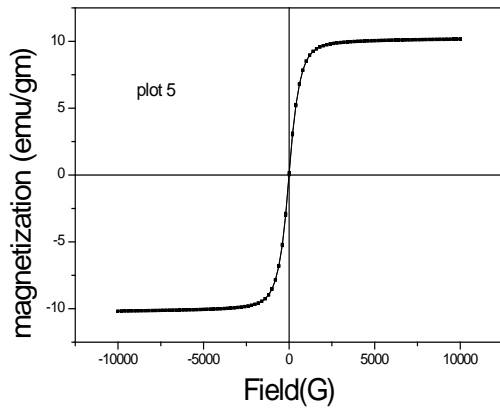
Plot 3. Zn ferrite Hysteresis plot for sample $\text{Cu}_{0.6}\text{Zn}_{0.4}\text{Fe}_2\text{O}_4$



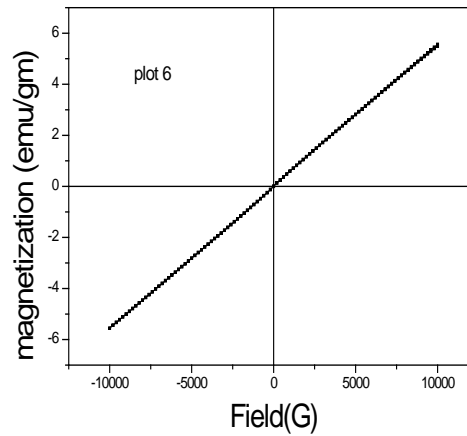
Plot 4. Zn ferrite Hysteresis plot for sample $\text{Cu}_{0.4}\text{Zn}_{0.6}\text{Fe}_2\text{O}_4$



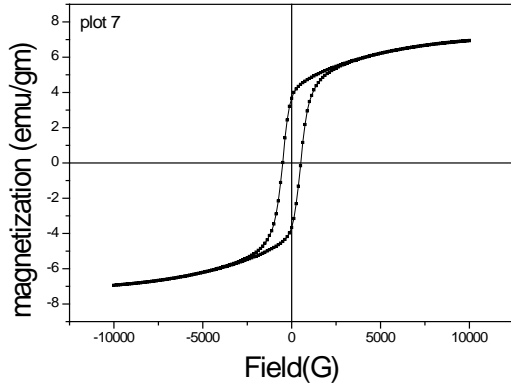
Plot 5. Zn ferrite Hysteresis plot for sample $\text{Cu}_{0.2}\text{Zn}_{0.8}\text{Fe}_2\text{O}_4$



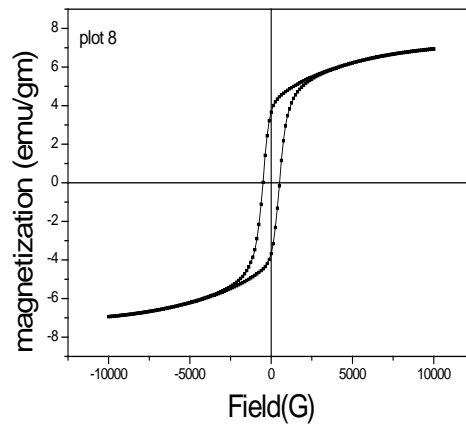
Plot 6. Zn ferrite Hysteresis plot for sample ZnFe_2O_4



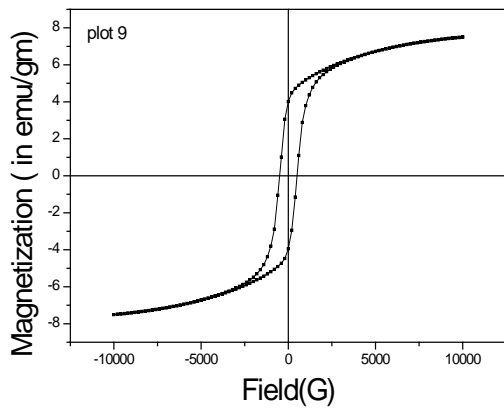
Plot 7. Cu Ferrite Hysteresis plot for CuFe_2O_4



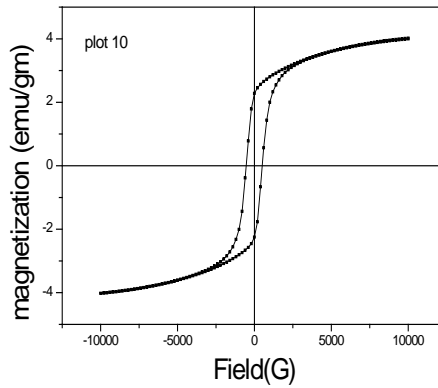
Plot 8. Sb Ferrite Hysteresis plot for $\text{Cu}_{0.8}\text{Sb}_{0.2}\text{Fe}_2\text{O}_4$



Plot 9. Sb Ferrite Hysteresis plot for $\text{Cu}_{0.6}\text{Sb}_{0.4}\text{Fe}_2\text{O}_4$



Plot 10. Sb Ferrite Hysteresis plot for $\text{Cu}_{0.4}\text{Sb}_{0.6}\text{Fe}_2\text{O}_4$



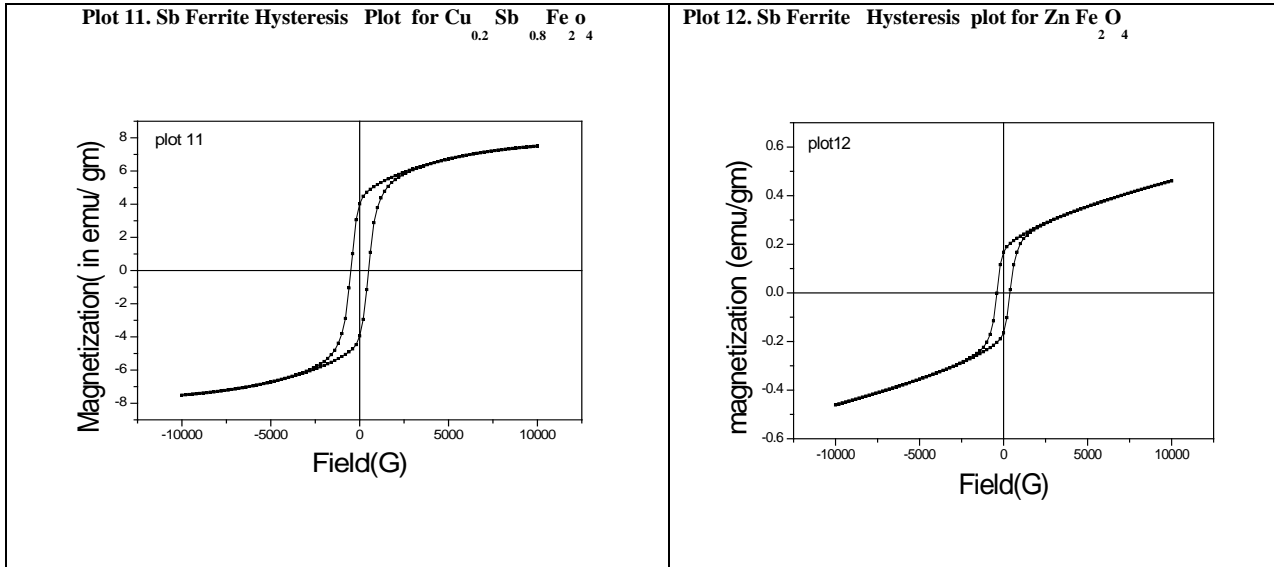


Table 1: Evaluated Domain Wall Energy Per Unit Area As a Function of Substituent Concentration

Serial No.	Substituent concentration	Domain wall energy (eV)	
		Sb	Zn
1	0.00	01.92	01.92
2	0.10	06.58	03.16
3	0.20	14.53	13.10
4	0.30	02.37	07.53
5	0.40	02.25	08.70
6	0.50	00.50	00.75

Table 2: The Variation of Magnetic Loss Factor ($\tan \mu_i$) with Additive Concentration

S.No.	Substituent conc. (x)	Magnetic loss factor	
		Sb	Zn
1	0.00	0.645	0.645
2	0.10	0.127	1.490
3	0.20	0.346	0.320
4	0.30	0.52	0.362
5	0.40	0.745	0.651
6	0.50	0.507	0.611

REFERENCES

[1] J. Smit and H.P.J Wijn (1959), ‘Ferrites’ Philips technical library (Netherlands) P150.

[2] L. Neel, (1948), Ann de Physics. 3, p 137.

[3] Maria Jose Benitez Romero,(2009),Ph.D. Dissertation on : ‘Self assembled Magnetic Nanostructures: Synthesis And Characterization’, submitted to der Ruhr Universitat , Bochum, Quito(Ecuador).

[4] J.M.Fert et.al. (1988),J.Phys.Rev.Lett 61,p2472 ; Ibid .,Phys. Rev.(1989),B39, p4828.

[5] J. Hubbard, (1963) Proc. Roy. Soc. A 276, p238.

[6] P. W. Anderson, (1961) Phys. Rev. 124, p41.

- [7] Liviu Hozoi, Ph.D., Thesis, (2003) 'Localized States in Transition Metal Oxides', submitted to: de Rijksuniversiteit, Groningen, Romania.
- [8] E. Dagotto, (1994) Rev. Mod. Phys. **66**, p763.
- [9] Hidetoshi Fukuyama, (2006), Rev. on: 'Physics of Molecular Conductors', J. Phys. Soc. Jpn. **75**, 051001
- [10] Yu-Wei Su., M.S., Thesis ,(2008), 'Fabrication and Characterization of Ferrimagnetic Film for RF/Microwave Crosstalk Suppression' , submitted to: Oregon State University, U.S.A.
- [11] Shenghui Guo, et.al., (2010) J. of Alloys and Compounds, **506**(1), 2010, pp L5-L7.
- [12] Pathan A.N. et.al., (2010), 'Synthesis, Characterisation and Magnetic Studies of $\text{Co}_{0.4}\text{Zn}_{(0.4-x)}\text{Cu}_x\text{Fe}_2\text{O}_4$ Nanoparticles', Abstracts of : Int.J. of Syst. Biology, ISSN: 0975-2900 & E-ISSN: 0975-9204, 2(1), p11, Copyright © 2010, Bio info Publications. Ibid: 'Synthesis and Mossbauer Studies on Nickel-Zinc- Copper Nano ferrites', Int.J. of Syst. Biology, ISSN: 0975-2900 & E-ISSN: 0975-9204, 2(1), p12, Copyright © 2010.
- [13] Kadam G.B. et.al., (2010) 'Effect of Zinc on A. C. Susceptibility and D. C. Resistivity of $\text{Ni}_{1-x}\text{Zn}_x\text{Fe}_{2-y}\text{Eu}_y\text{O}_4$ ', Abstracts of : Int.J. of Syst. Biology, ISSN: 0975-2900 & E-ISSN: 0975-9204, 2(1), p12 ; Ibid: 'Structural and electrical properties of SM3+ doped Co- Zn ferrite', Abstracts of : Int.J. of Syst. Biology, ISSN: 0975-2900 & E-ISSN: 0975-9204, 2(1); p12.
- [14] E. Dagotto, (1994) Rev. Mod. Phys. **66**, p763.
- [15] M. A. SOLOMAN (2002), Ph.D. Thesis entitled , "Evaluation of Magnetic Dielectric and ... Ferrite composites" , submitted to Cochin University Of Science and Technology, Cochin -682022, INDIA
- [16] Yu-Wei Su., M.S., Thesis ,(2008), 'Fabrication and Characterization of Ferri magnetic Film RF/Microwave Crosstalk Suppression' , submitted to: Oregon State University, U.S.A
- [17] R. Dhanaraju et.al. (2011), "Measurements of Electrical characteristics of Zn & Sb substituted Cu ferrites, and the frequency dependence of resistivity for Zn substituted Cu ferrite" in 'SCIENCE & SOCIETY' (ISSN 0973-0206), Proc. Of. Nat. Sym. on Nano.Sci. and Tech-2011.9(2), pp 97-102
- [18] R. Dhanaraju et.al., (2011), 'SEM and XRD studies on Sb substituted Cu ferrite nanomaterial' in 'SCIENCE & SOCIETY' (ISSN 0973-0206) , Proc. Of. Nat. Sym. on Nano.Sci. and Tech-2011.9(2), pp 103-108
- [19] R. Dhanaraju et.al. (2011), 'Graphical traits about VHTM in the light of FTIR Studies on Zn & Sb substituted Cu ferrites' , International Journal of Engineering Science and Technology, **3** (11), pp. 8058-8064
- [20] Fursina. A.A. (2010): Ph.D. Thesis entitled: 'Investigation of Electrically Driven Transition in Magnetite, Fe_3O_4 , Nanostructures', submitted to Rice University, Houston, Texas, U.S.A.,
- [21] E Manova et.al., (2010), 'Characterization of nanodimensional Ni-Zn ferrite prepared by mechanochemical and thermal methods' , Journal of Physics: Conference Series **217** (2010) 012102, International Conference on the Applications of the Mössbauer Effect (ICAME 2009), IOP Publishing.
- [22] S. Deka et.al., (2006), 'Characterization of nanosized NiZn ferrite powders synthesized by an autocombustion method', Materials Chemistry and Physics, **100**(1), pp 98-101
- [23] Mei Yu et.al., (2007), 'Fabrication and characterization of highly ordered $\text{Ni}_0.5\text{Zn}_0.5\text{Fe}_2\text{O}_4$ nanowire/tube arrays by sol-gel template method', Journal of University of Science and Technology Beijing, Mineral, Metallurgy, Material. **14**(5), Pages 469-472.
- [24] R. L. Dhiman et al., (2008), 'Preparation and Characterization of Manganese Ferrite Aluminates', Advances in Condensed Matter Physics, vol2008 , article ID703479, 7Pages .
- [25] Joaquin Garcia et.al., (2004), Topical Review on 'The Verwey transition—a new perspective', J. Phys.: Condens. Matter **16** (2004) R145–R178.
- [26] Kadam G.B. et.al., (2010) , Journal of Electronic and Electrical Engineering, (ISSN: 0976-8106 & E-ISSN: 0976-8114) , **1**(1), PP-15-25
- [27] R.N. Bhowmik et.al., (2010), International Journal of Engineering, Science and Technology, ISSN: 0975-5462, 2(8), pp. 40-52

- [28] A.M. Bhavikatti (2011) , International Journal of Engineering Science and Technology ISSN: 0975-5462 , (IJEST),3(1),pp 657-695
- [29] C. Venkatarajua (2010), Journal of Alloys and Compounds, 498 (2) , pp203-206
- [30] Carolyn I. Pearce et.al, (2010), '*Iron site occupancies in magnetite-ulvospinel solid solution: A new approach using XMCD*', *LBNL Paper LBNL-3328E*, '*e Scholarship*' ,University of California
- [31] S.R.Sawant et.al., (1981), '*Magnetic hysteresis studies on slow cooled and quenched $\text{Cu}_x\text{Zn}_{1-x}\text{Fe}_2\text{O}_4$ system*', in Solid State Communications, **40(4)**, pp 391-394.
- [32] Shun Hua Xiao et.al., (2007) , '*Low-temperature auto-combustion synthesis and magnetic properties of cobalt ferrite nanopowder*', in Materials Chemistry and Physics, **106(1)**, PP82-87.
- [33] S. Nakayama. et al (1968) J. Phys. Soc. Jap 24 (1968) 219.
- [34] B.G. Landa,et.al.,(1999), Solid state commn., **110** ,p 435.
- [35] A.W. Sleight, et.al., (1972) J.Phys. Chem. Solids 33 p679.
- [36] J.B. Goodenough, (1963)'Magnetism and Chemical Bond' , Wiley, New York .
- [37] K.I.Kobayasy et al.,(1998) Nature 395 p 677.
- [38] K.S. Lakshmi, et.al.(1998), J.Mag. Soc. Of Japan, 22 suppl. No.S1p 37.